RESEARCH　　　　　　　　　　　　　　　　　　　　　　　**Open Access**

Two-stage decoding algorithm for unmodulated parallel combinatory high-compaction multicarrier modulation signals

Ryuji Hayashi, Yingsong Li[*] and Masanori Hamamura

Abstract

A new decoding algorithm that consists of two decoding stages to reduce the computational complexity of maximum likelihood decoding for parallel combinatory high-compaction multicarrier modulation is proposed. The first decoding stage is responsible for a preliminary decision that serves to roughly find candidate messages using the QRD-M algorithm, and the second decoding stage is responsible for the final decision that reduces the error contained in the candidate and determines the message using the minimum value of the Hamming distances between the candidate and the replicas of the message. The complexity is considerably reduced by the proposed two-stage decoding algorithm at a cost of approximately 1.5 dB or less in E_b/N_0 with respect to the bit-error rate of 10^{-3} under the given parameter settings.

Keywords: PC signaling, HC-MCM, QRD-M algorithm, Maximum likelihood decoding

1 Introduction

Recently, multicarrier transmission systems have been investigated from the viewpoint of high-speed communication and high spectral efficiency for wireless communication. Orthogonal frequency-division multiplexing (OFDM) is a well-known multicarrier transmission system that has a high transmission rate and high resistance to multipath interference over the multipath channel [1-3]. On the other hand, parallel combinatory (PC) signaling methods have been investigated as methods for improving spectral efficiency [4-8]. Parallel combinatory OFDM (PC-OFDM) was proposed in a previous article [9] and uses the technique of PC signaling, which has higher spectral efficiency and a lower bit-error rate (BER) than ordinary OFDM. Another technique that improves the spectral efficiency of OFDM is high-compaction multicarrier modulation (HC-MCM) [10]. This is a method of achieving high spectral efficiency by overlapping the carriers of the transmitted signal. Parallel combinatory

HC-MCM (PC/HC-MCM) [11] was proposed using the techniques of PC signaling and HC-MCM. Parallel combinatory HC-MCM can be categorized as either modulated PC/HC-MCM or unmodulated PC/HC-MCM. Modulated PC/HC-MCM transmits a truncated PC-OFDM signal, which is a PC-OFDM signal multiplied by a window function in the time domain, and improves the BER performance of HC-MCM. Unmodulated PC/HC-MCM transmits a truncated PC-OFDM signal without N-ary amplitude phase shift keying (APSK) modulation and improves the peak-to-average power ratio (PAR) of HC-MCM. In both types of PC/HC-MCM, the transmission rate can be chosen flexibly by controlling the window width, which changes the modulation index of PC/HC-MCM. Therefore, PC/HC-MCM can be designed to have a lower PAR and higher spectrum efficiency than conventional OFDM and is suitable for consumer electronic device applications, such as sensor networks and wireless home networks. PC/HC-MCM is also compatible with the conventional OFDM used in wireless multimedia, digital audio/video broadcasting (DAB/DVB), and so forth.

Maximum likelihood (ML) decoding [12] has been considered as a means of recovering message data with

*Correspondence: 156011y@gs.kochi-tech.ac.jp
Graduate School of Engineering, Kochi University of Technology, Kami-shi 782-8502, Japan

a lower BER in PC/HC-MCM. However, the computational complexity for demodulation using ML decoding increases with the number of combinations of PC signaling. An effective method that reduces the computational complexity for ML decoding is to reduce the number of Euclidean distance calculations required to identify the transmitted message data using the (M)-algorithm at the receiver [13,14].

In this article, a method using the QRD-M algorithm [15,16], which uses QR decomposition (QRD) and the (M)-algorithm [17] to improve the demodulation efficiency of PC/HC-MCM, is proposed and its performance is verified over an additive white Gaussian noise (AWGN) channel. This algorithm consists of two decoding stages. The first decoding stage is responsible for a preliminary decision that serves to roughly find candidate message data using the QRD-M algorithm. The second decoding stage is responsible for a final decision that corrects the error contained in the candidate decoded at the first decoding stage. Although another type of two-stage decoding algorithm has been considered [18], we have modified it to more efficiently and reliably decode the message data.

The remainder of this article is organized as follows. In Section 2, PC-OFDM and unmodulated PC/HC-MCM are introduced and ML decoding is formulated. In Section 3, the proposed decoding algorithm is described. In Section 4, the computational complexity and BER performance of PC/HC-MCM using the proposed decoding algorithm are discussed. Finally, this article is concluded in Section 5.

2 Unmodulated PC/HC-MCM
2.1 PC-OFDM
PC-OFDM is a type of OFDM that conveys message data with PC signaling together with ordinary N-ary amplitude and phase shift keying (N-ary APSK).

Let M_c be the total number of preassigned carriers and M_p be the number of carriers selected for PC signaling. In this case, the number of message data bits per PC-OFDM signal, m_{total} [bits], is represented as

$$m_{\text{total}} = m_{\text{apsk}} + m_{pc}, \tag{1}$$

where m_{apsk} [bits] is the number of message data bits mapped into N-ary APSK constellations of M_p carriers, given by

$$m_{\text{apsk}} = M_p \log_2 N, \tag{2}$$

and m_{pc} [bits] is the number of message data bits encoded into one of the prescribed sets of M_p carriers, that is,

$$m_{pc} = \left\lfloor \log_2 \binom{M_c}{M_p} \right\rfloor, \tag{3}$$

where $\lfloor \cdot \rfloor$ is an operator that denotes the largest integer that is smaller than or equal to the operand.

The PC-OFDM signals are modeled as

$$y(t) = \sum_{l=1}^{M_c} x_l e^{j2\pi(l-1)\Delta f t}, \quad 0 \leqq t < T_0, \tag{4}$$

where x_l $(l = 1, 2, \ldots, M_c)$ is the complex symbol for the lth carrier, which takes an $(N+1)$-ary APSK constellation including zero amplitude; in $0 \leqq t < T_0$, $T_0 = 1/\Delta f$ [s] is the duration of one PC-OFDM signal and Δf [Hz] is the frequency spacing.

Here, m_{pc} message data bits can be transmitted without N-ary APSK in PC-OFDM. In this case, $x_l \in \{0, 1\}$ and $m_{\text{total}} = m_{pc}$.

2.2 PC/HC-MCM
Similarly to PC-OFDM, PC/HC-MCM is a multicarrier modulation scheme that uses PC signaling. PC/HC-MCM can be categorized as either modulated PC/HC-MCM or unmodulated PC/HC-MCM. Modulated PC/HC-MCM transmits a truncated PC-OFDM signal, and unmodulated PC/HC-MCM transmits a truncated PC-OFDM signal without N-ary APSK modulation. In this article, we consider unmodulated PC/HC-MCM to take advantage of one of its favorable properties. For example, we can choose $\binom{M_c}{M_p} = \binom{16}{8}$ and modulation index 0.5 to transmit 13 bits message data. This means that the unmodulated PC/HC-MCM system can transmit 13 bits data within a time duration of $0.5T_0$ using 16 Δf bandwidth. In other words, the unmodulated PC/HC-MCM system can transmit $2 \times 13 = 26$ bits within $1T_0$ using 16 Δf bandwidth, which indicates that the spectral efficiency of the unmodulated PC/HC-MCM system is better than that of the OFDM with BPSK which can transmit only 16 bits within $1T_0$ using 16 Δf bandwidth. We hereinafter refer to unmodulated PC/HC-MCM simply as PC/HC-MCM.

Let $\mathcal{A} = \{k \in \mathbb{N} \mid 1 \leqq k \leqq M_c\}$ be the set of frequency indices of all preassigned carriers, and let $\mathcal{B} = \{b_1, b_2, \ldots, b_{M_p}\} \subset \mathcal{A}(|\mathcal{B}| = M_p$, where $|\cdot|$ is the cardinality, that is, the number of elements in the set) be a subset of $\mathcal{A}$, which is the set of the frequency indices of carriers used for PC signaling. Without loss of generality, we assume that $b_1 < b_2 < \cdots < b_{M_p}$. Note that $\mathcal{B}$ is a possible subset of $\mathcal{A}$, that is, $\mathcal{B} \in \mathcal{C} = \{\mathcal{B}_1, \mathcal{B}_2, \ldots, \mathcal{B}_{2^{m_{pc}}}\}$. In this case, the PC/HC-MCM signal can be written in a complex low-pass equivalent notation as

$$y(t) = w(t) \sum_{l \in \mathcal{B}} e^{j2\pi(l-1)\Delta f t}, \quad 0 \leqq t < T_s, \tag{5}$$

where T_s is the duration [s] and is chosen to be $T_s < 1/\Delta f$ for PC/HC-MCM, and $w(t)$ is a window function defined in $0 \leqq t < T_s$. In this article, $w(t)$ is assumed to be $w(t) = \sin(\frac{\pi}{T_s}t)$, which is a finite-duration window that minimizes the root mean square (RMS) bandwidth of each carrier that is transmitted [19].
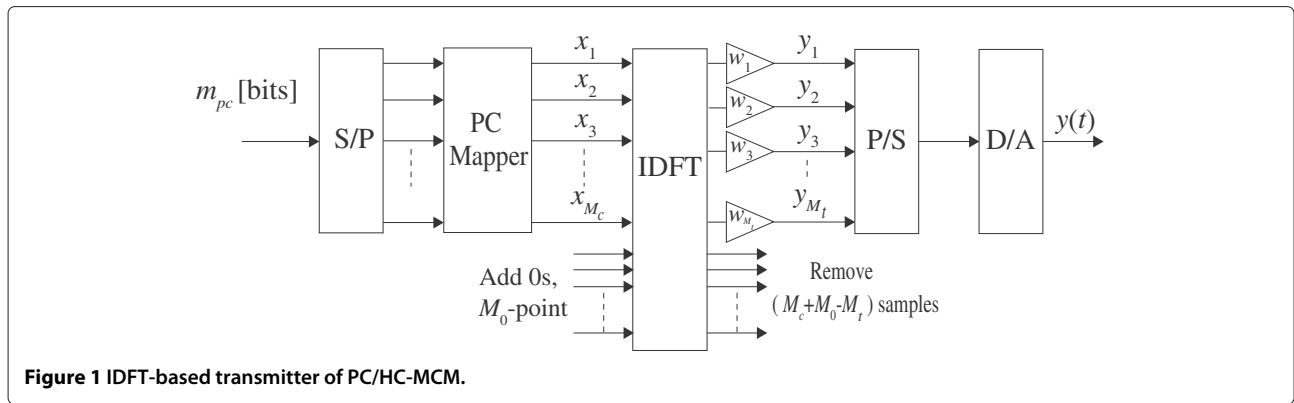
Figure 1 IDFT-based transmitter of PC/HC-MCM.

The above expression can be rewritten as

$$y(t) = w(t) \sum_{l=1}^{M_c} x_l e^{j2\pi(l-1)\Delta ft}, \quad 0 \leqq t < T_s, \qquad (6)$$

where

$$x_l = \begin{cases} 1 & (l \in \mathcal{B}) \\ 0 & (l \notin \mathcal{B}) \end{cases}. \qquad (7)$$

Therefore, an inverse discrete Fourier transform (IDFT) transmitter for PC/HC-MCM can be configured using (6) as shown in Figure 1. At the transmitter, m_{pc} message data bits are subjected to serial-to-parallel (S/P) conversion and are mapped into one of the possible $2^{m_{pc}}$ combinations of M_p carriers, the frequencies of which are characterized by the set $\mathcal{B}$ of frequency indices. An example of PC mapping using the Gray code for $\binom{M_c}{M_p} = \binom{8}{2}$ is given in Table 1.

At the transmitter of PC/HC-MCM, M_0 zeros are tacked onto the binary sequence x_l ($l = 1, 2, \ldots, M_c$) as padding at the input of the IDFT for the interpolation of discrete-time samples obtained by the IDFT. After the IDFT, we obtain $M_c + M_0$ samples and remove ($M_c + M_0 - M_t$) samples. Therefore, only M_t samples, weighted by gain constants $w_m = \sin\left(\frac{m-1}{M_t}\pi\right)$ ($m = 1, 2, \ldots, M_t$), are used for parallel-to-serial (P/S) conversion and digital-to-analog (D/A) conversion to produce the transmitting signal $y(t)$.

At the receiver shown in Figure 2, the signal $y(t)$ is detected in the presence of an AWGN $n(t)$ with a double-sided power spectral density of $N_0/2$. After the A/D converter, we obtain the discrete-time samples $\hat{y}_m$ ($m = 1, 2, \ldots, M_t$) detected at time $t = (m-1)T_s/M_t$, that is,

$$\hat{y}_m = (y(t) + \eta(t))_{t=(m-1)T_s/M_t}, \qquad (8)$$

where $\eta(t)$ is the noise obtained at the A/D converter output.

Let $\hat{\mathbf{y}}$ be a column vector that contains the samples $\hat{y}_m$ such that

$$\hat{\mathbf{y}} = [\hat{y}_1 \; \hat{y}_2 \; \cdots \; \hat{y}_{M_t}]^T, \qquad (9)$$

and let $\mathbf{x}_\mathcal{B} = [x_1 \; x_2 \; \ldots \; x_{M_c}]^T$ be a column vector that has the elements x_l defined as (7). The IDFT transmitter is expressed by the submatrix $\mathbf{F}$ of the full IDFT matrix, given by

$$\mathbf{F} = \begin{bmatrix} \omega_{1,1} & \cdots & \omega_{1,M_c} \\ \vdots & \ddots & \vdots \\ \omega_{M_t,1} & \cdots & \omega_{M_t,M_c} \end{bmatrix}, \qquad (10)$$

where

$$\omega_{m,l} = \frac{1}{\sqrt{M_c + M_0}} e^{j\frac{2\pi(l-1)(m-1)}{M_c+M_0}}. \qquad (11)$$

Therefore, $\hat{\mathbf{y}}$ is expressed using $\mathbf{F}$ and $\mathbf{x}_\mathcal{B}$ as

$$\hat{\mathbf{y}} = \mathbf{W}\mathbf{F}\mathbf{x}_\mathcal{B} + \boldsymbol{\eta}, \qquad (12)$$

Table 1 Example of PC mapping using the Gray code for $\binom{M_c}{M_p} = \binom{8}{2}$

| Message data	$\mathcal{B}_i$	Frequencies	$\mathbf{x}_{\mathcal{B}_i} = [x_{i,1} x_{i,2} \ldots x_{i,8}]^T$
1100	{1,2}	$\{f_1, f_2\}$	$[1\,1\,0\,0\,0\,0\,0\,0]^T$
1101	{1,3}	$\{f_1, f_3\}$	$[1\,0\,1\,0\,0\,0\,0\,0]^T$
1111	{1,4}	$\{f_1, f_4\}$	$[1\,0\,0\,1\,0\,0\,0\,0]^T$
1110	{1,5}	$\{f_1, f_5\}$	$[1\,0\,0\,0\,1\,0\,0\,0]^T$
1010	{1,6}	$\{f_1, f_6\}$	$[1\,0\,0\,0\,0\,1\,0\,0]^T$
1011	{1,7}	$\{f_1, f_7\}$	$[1\,0\,0\,0\,0\,0\,1\,0]^T$
1001	{1,8}	$\{f_1, f_8\}$	$[1\,0\,0\,0\,0\,0\,0\,1]^T$
1000	{2,3}	$\{f_2, f_3\}$	$[0\,1\,1\,0\,0\,0\,0\,0]^T$
0000	{2,4}	$\{f_2, f_4\}$	$[0\,1\,0\,1\,0\,0\,0\,0]^T$
0001	{2,5}	$\{f_2, f_5\}$	$[0\,1\,0\,0\,1\,0\,0\,0]^T$
0011	{2,6}	$\{f_2, f_6\}$	$[0\,1\,0\,0\,0\,1\,0\,0]^T$
0010	{2,7}	$\{f_2, f_7\}$	$[0\,1\,0\,0\,0\,0\,1\,0]^T$
0110	{2,8}	$\{f_2, f_8\}$	$[0\,1\,0\,0\,0\,0\,0\,1]^T$
0111	{3,4}	$\{f_3, f_4\}$	$[0\,0\,1\,1\,0\,0\,0\,0]^T$
0101	{3,5}	$\{f_3, f_5\}$	$[0\,0\,1\,0\,1\,0\,0\,0]^T$
0100	{3,6}	$\{f_3, f_6\}$	$[0\,0\,1\,0\,0\,1\,0\,0]^T$
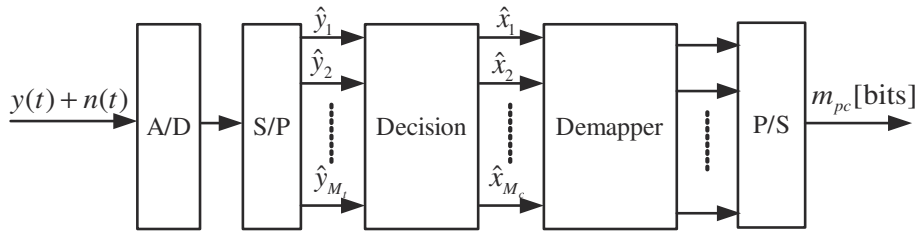
Figure 2 Receiver of PC/HC-MCM.

where η is a column vector that contains the samples of the noise term $\eta(t)$ and $\mathbf{W}$ is a diagonal matrix that has the weights w_m ($m = 1, 2, \ldots, M_t$) in its main diagonal, that is,

$$\mathbf{W} = \mathrm{diag}\{w_1, w_2, \ldots, w_{M_t}\}. \tag{13}$$

2.3 Maximum likelihood decoding

The decision stage determines which PC/HC-MCM signal, characterized by the set $\mathcal{B}$ of indices of carriers, was transmitted. In this problem, from all possible sets of $\mathcal{B}_i \in \mathcal{C}$, ML decoding finds the set $\hat{\mathcal{B}}$ that satisfies the following formula:

$$\hat{\mathcal{B}} = \arg\min_{\mathcal{B}_i \in \mathcal{C}}(J(\mathcal{B}_i) = ||\hat{\mathbf{y}} - \mathbf{WF}\mathbf{x}_{\mathcal{B}_i}||), \tag{14}$$

where $\mathbf{WF}\mathbf{x}_{\mathcal{B}_i}$ ($i = 1, 2, \ldots, 2^{m_{pc}}$) are the replica vectors, that is, the noiseless version of vector $\hat{\mathbf{y}}$, and $||\cdot||$ denotes the Euclidean norm of the enclosed vector.

Maximum likelihood decoding is an optimization method that minimizes the probability of an error in finding the set $\mathcal{B}$ used to transmit the PC/HC-MCM signal. However, since the value of $2^{m_{pc}}$ is a very large integer when $\binom{M_c}{M_p}$ is large, it is difficult to solve such a problem for $M_c \gg 1$ and $M_p \approx M_c/2$.

3 Two-stage decoding algorithm

To reduce the complexity of ML decoding, a decoding algorithm that consists of two decoding stages is proposed. The first decoding stage is responsible for a preliminary decision that serves to roughly find the likely candidates of $\mathcal{B}$ using the QRD-M algorithm. The second decoding stage is responsible for a final decision to recover the message data, which selects the most likely

candidate among those determined using the results of the first decoding stage.

3.1 First decoding stage

The QRD-M algorithm is a technique that uses QR decomposition combined with the (M)-algorithm to reduce the complexity of ML decoding. A block diagram of the transmitter and receiver of PC/HC-MCM discussed in this article is shown in Figure 3.

The QR decomposition of the matrix $\mathbf{WF}$ is given by

$$\mathbf{WF} = \mathbf{QR}, \tag{15}$$

where $\mathbf{Q}$ is the $M_t - \mathrm{by} - M_t$ unitary matrix ($\mathbf{Q}^H = \mathbf{Q}^{-1}$)

$$\mathbf{Q} = \begin{bmatrix} q_{1,1} & \cdots & q_{1,M_t} \\ \vdots & \ddots & \vdots \\ q_{M_t,1} & \cdots & q_{M_t,M_t} \end{bmatrix}, \tag{16}$$

and $\mathbf{R}$ is the M_t-by-M_c upper triangular matrix

$$\mathbf{R} = \begin{bmatrix} a_{1,1} & a_{1,2} & \cdots & a_{1,M_c-1} & a_{1,M_c} & (1) \\ 0 & a_{2,2} & \cdots & a_{2,M_c-1} & a_{2,M_c} & (2) \\ \vdots & \vdots & \ddots & \vdots & \vdots & \vdots \\ 0 & 0 & \cdots & a_{M_c-1,M_c-1} & a_{M_c-1,M_c} & (M_c-1)\cdot \\ 0 & 0 & \cdots & 0 & a_{M_c,M_c} & (M_c) \\ \vdots & \vdots & \ddots & \vdots & \vdots & \vdots \\ 0 & 0 & \cdots & 0 & 0 & (M_t) \end{bmatrix} \tag{17}$$

By premultiplying the received signal vector $\hat{\mathbf{y}}$ by the matrix $\mathbf{Q}^H$, we obtain

$$\mathbf{Q}^H\hat{\mathbf{y}} = \mathbf{Q}^H(\mathbf{WF}\mathbf{x}_{\mathcal{B}} + \eta) = \mathbf{R}\mathbf{x}_{\mathcal{B}} + \mathbf{Q}^H\eta. \tag{18}$$
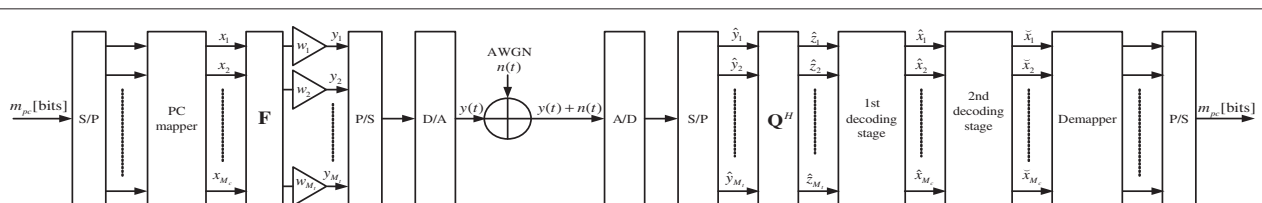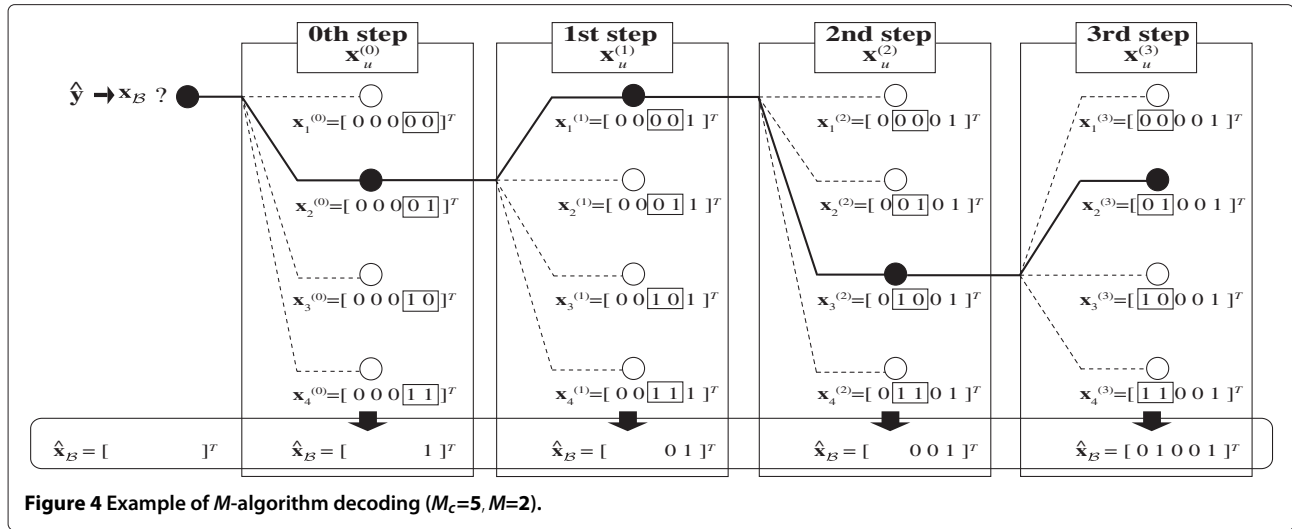

Figure 3 Block diagram of proposed PC/HC-MCM.

Figure 4 Example of *M*-algorithm decoding ($M_c=5$, $M=2$).

Since $\mathbf{Q}^H\mathbf{y} = \mathbf{R}\mathbf{x}_{\mathcal{B}}$ for the noiseless vector $\mathbf{y}$ of $\hat{\mathbf{y}}$, this formula can be used to produce replica vectors $\mathbf{R}\mathbf{x}_{\mathcal{B}_i}$ ($\mathcal{B}_i \in \mathcal{C}$) such that

$$
\mathbf{R}\mathbf{x}_{\mathcal{B}_i} = \begin{bmatrix} a_{1,1}\,x_{i,1} + \cdots + a_{1,M_c}\,x_{i,M_c} \\ \vdots \\ \vdots \\ \vdots \\ a_{M_c-1,M_c-1}\,x_{i,M_c-1} + a_{M_c-1,M_c}\,x_{i,M_c} \\ a_{M_c,M_c}\,x_{i,M_c} \\ 0 \\ \vdots \\ 0 \end{bmatrix} \begin{matrix} (1) \\ \vdots \\ \vdots \\ \vdots \\ (M_c-1), \\ (M_c) \\ \\ \\ \vdots \\ (M_t) \end{matrix}
\tag{19}
$$

where $x_{i,l}$ ($l = 1, 2, \ldots, M_c$) is the lth element of vector $\mathbf{x}_{\mathcal{B}_i}$.

To reduce the number of replica vectors $\mathbf{R}\mathbf{x}_{\mathcal{B}_i}$, the proposed method using the (M)-algorithm uses vectors $\mathbf{x}_u^{(0)}$ ($u = 1, 2, \ldots, U_0 \leq 2^M$) that contain all possible limited M elements of $\mathbf{x}_{\mathcal{B}_i}$ at the 0th step[a].

$$
\mathbf{x}_u^{(0)} = [\; \overbrace{0 \; \cdots \; 0}^{M_c-M \text{ zeros}} \; \overbrace{x_{u,M_c-M+1}^{(0)} \cdots x_{u,M_c}^{(0)}}^{M \text{ elements}}]^T
\tag{20}
$$

Therefore, using $\mathbf{x}_u^{(0)}$, it is expected that a candidate $\hat{x}_{M_c}$ of x_{M_c} can be efficiently estimated such that

$$
\hat{x}_{M_c} = x_{u_0,M_c}^{(0)}, \qquad u_0 = \arg\min_u \left(||\mathbf{Q}^H\hat{\mathbf{y}} - \mathbf{R}\mathbf{x}_u^{(0)}|| \right).
\tag{21}
$$

Vectors $\mathbf{x}_u^{(1)}$ ($u = 1, 2, \ldots, U_1 \leq 2^M$) are defined using $\hat{x}_{M_c}$ obtained at the 0th step as

$$
\mathbf{x}_u^{(1)} = [\; \overbrace{0 \; \cdots \; 0}^{M_c-M-1 \text{ zeros}} \; \overbrace{x_{u,M_c-M}^{(1)} \cdots x_{u,M_c-1}^{(1)}}^{M \text{ elements}} \; \hat{x}_{M_c}]^T, \tag{22}
$$
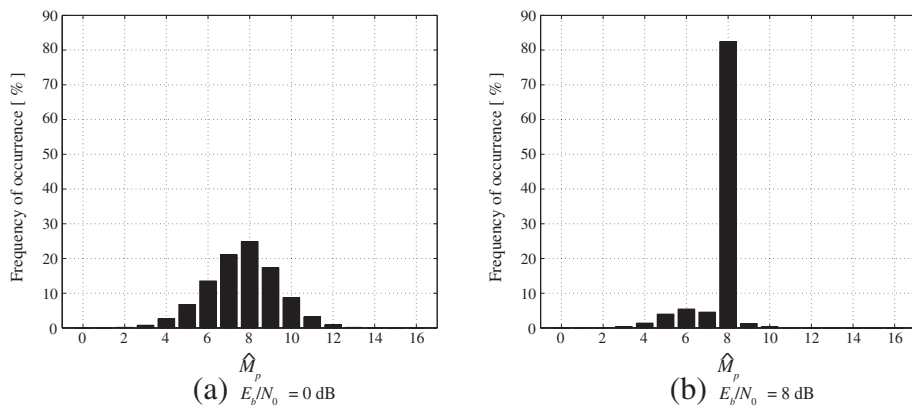
Figure 5 Histogram of the Hamming weight of $\hat{x}_{\mathcal{B}}$ $\left(\binom{M_c}{M_p} = \binom{16}{8}\right)$, $\Delta f T_s = 0.5$, $M = 7$). (**a**) $E_b/N_0 = 0$ dB. (**b**) $E_b/N_0 = 8$ dB.

Figure 6 Histogram of the minimum Hamming distance $d_{\min}$ between vectors $\hat{x}_{\mathcal{B}}$ and $x_{\mathcal{B}_i \in \mathcal{C}}$ $\left(\binom{M_c}{M_p} = \binom{16}{8}, \Delta f T_s = 0.5 \right)$. (a) $E_b/N_0 = 0$ dB.
(b) $E_b/N_0 = 8$ dB.
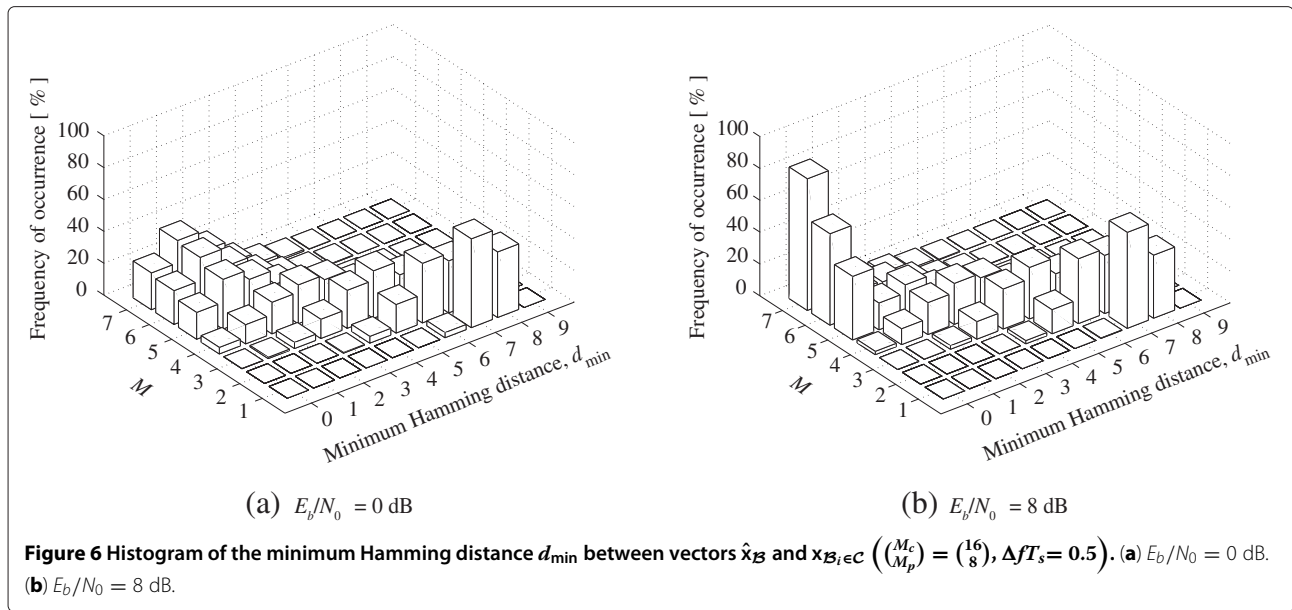
and a candidate $\hat{x}_{M_c-1}$ of x_{M_c-1} is obtained such that

$$\hat{x}_{M_c-1} = x_{u_1,M_c-1}^{(1)}, \quad u_1 = \arg \min_u \left(||\mathbf{Q}^H \hat{\mathbf{y}} - \mathbf{R} \mathbf{x}_u^{(1)}|| \right) \tag{23}$$

at the first step. Similarly, at the nth step ($n = 0, 1, \ldots, M_c - M - 1$), we obtain $\hat{x}_{M_c-n}$ using vectors $\mathbf{x}_u^{(n)}$ ($u = 1, 2, \ldots, U_n \leq 2^M$) given by

$$\mathbf{x}_u^{(n)} = [\overbrace{0 \ \ldots \ 0}^{M_c-M-n \text{ zeros}} \overbrace{x_{u,M_c-M-n+1}^{(n)} \cdots x_{u,M_c-n}^{(n)}}^{M \text{ elements}} \hat{x}_{M_c-n+1} \ldots \hat{x}_{M_c}]^T, \tag{24}$$

such that

$$\hat{x}_{M_c-n} = x_{u_n,M_c-n}^{(n)}, \quad u_n = \arg \min_u \left(||\mathbf{Q}^H \hat{\mathbf{y}} - \mathbf{R} \mathbf{x}_u^{(n)}|| \right). \tag{25}$$

At the $(M_c - M)$th step, we simultaneously obtain the candidates $\hat{x}_1, \ldots, \hat{x}_M$. Therefore, $\hat{x}_1$ is obtained at the $(M_c - M)$th step, and, after performing all of the above steps, we finally have $\hat{\mathbf{x}}_{\mathcal{B}} = [\hat{x}_1 \ \hat{x}_2 \ \ldots \ \hat{x}_{M_c}]^T$.

An example of the (M)-algorithm for $M_c = 5$ and $M = 2$ is illustrated in Figure 4. Note that the computational complexity for the first decoding stage is deterministic if the parameter M is fixed at the receiver.
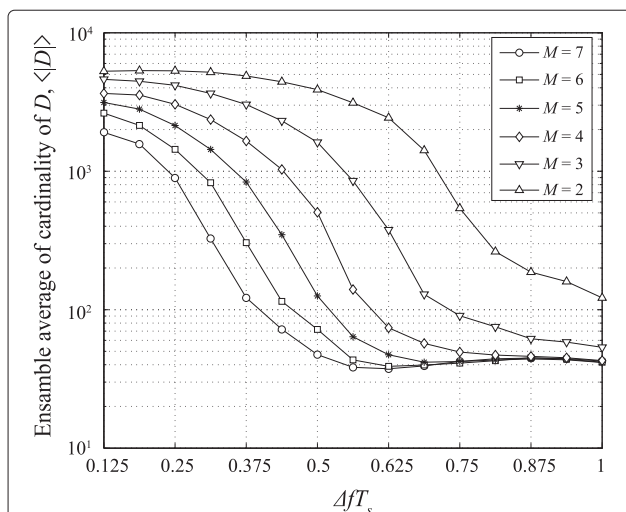
3.2 Second decoding stage

The primary purpose of the second decoding stage shown in Figure 3 is to solve the problem that the number of nonzero elements (ones), $\hat{M}_p$ (the Hamming weight), contained in the vector $\hat{\mathbf{x}}_{\mathcal{B}}$ is not necessarily equal to the integer M_p adopted for PC signaling.

Table 2 Specifications of the simulations

System item	Parameter
$\binom{M_c}{M_p}$, m_{pc}	$\binom{16}{8}$, 13
M	2, 3, 4, 5, 6, 7
M_t	32
Window	Half-wave sinusoid
PC mapping	Gray code mapping
Noise	AWGN
Synchronization	Complete

Figure 7 Complexity of the second decoding stage
$\left(\binom{M_c}{M_p} = \binom{16}{8}, E_b/N_0 = 8 \text{ dB} \right)$.

Figure 5 shows examples of histograms obtained through simulations for $\binom{M_c}{M_p} = \binom{16}{8}$, $\Delta f T_s = 0.5$, and $M = 7$. In Figure 5a, E_b/N_0 was chosen to be 0 dB, and in Figure 5b, E_b/N_0 was chosen to be 8 dB, where E_b is the average energy per bit of the PC/HC-MCM signals. Although the most frequently occurring value of $\hat{M}_p$ is 8 ($= M_p$), the probability that $\hat{M}_p$ takes different integers is not negligible. This means that the vector $\hat{\mathbf{x}}_{\mathcal{B}}$ obtained at the first decoding stage is not necessarily included in the possible set of vectors $\mathbf{x}_{\mathcal{B}_i \in \mathcal{C}}$, which directly results in an increase in the BER. Therefore, we use the second decoding stage to reduce the error contained in $\hat{\mathbf{x}}_{\mathcal{B}}$. In the second decoding stage, we use the Hamming distances $d_H(\hat{\mathbf{x}}_{\mathcal{B}}, \mathbf{x}_{\mathcal{B}_i \in \mathcal{C}})$ between vectors $\hat{\mathbf{x}}_{\mathcal{B}}$ and $\mathbf{x}_{\mathcal{B}_i \in \mathcal{C}}$ to search for a subset $\mathcal{D} \subset \mathcal{C}$, which corresponds to the set of vectors $\mathbf{x}_{\mathcal{B}_i \in \mathcal{D}}$ that have the minimum value $d_{\min}$ of the Hamming distances $d_H(\hat{\mathbf{x}}_{\mathcal{B}}, \mathbf{x}_{\mathcal{B}_i \in \mathcal{C}})$. In the second decoding stage, all the vectors $\mathbf{x}_{\mathcal{B}_i \in \mathcal{C}}$ are compared with $\hat{\mathbf{x}}_{\mathcal{B}}$ to obtain the subset $\mathcal{D}$. This involves logical computations, which require fewer computations than the multiplications involved in the Euclidean distance calculations.

Figure 6 shows histograms of the minimum Hamming distance $d_{\min}$ for various values of the parameter M in the (M)-algorithm. In Figure 6a, E_b/N_0 was chosen to be 0 dB, and in Figure 6b, E_b/N_0 was chosen to be 8 dB. Figure 6a,b show that the minimum Hamming distance $d_{\min}$ depends greatly on the values of M and E_b/N_0. However, for high E_b/N_0 and $M \geq 5$, $d_{\min} = 0$ occurs with higher probability. In such a case, the computational complexity is not strongly affected by the second decoding stage, because the second decoding stage does not work for $d_{\min} = 0$. However, the computational complexity of the first decoding stage increases with the value of M.

Using the subset $\mathcal{D}$, the second decoding stage decodes the message data such that

$$\check{\mathbf{x}}_{\mathcal{B}} = \arg \min_{\mathcal{B}_i \in \mathcal{D}} \left(||\mathbf{Q}^H \hat{\mathbf{y}} - \mathbf{R} \mathbf{x}_{\mathcal{B}_i}|| \right). \tag{26}$$

4 Results
4.1 Computational complexity
As mentioned in Section 3.1, the computational complexity of the first decoding stage is deterministic, whereas that of the second decoding stage is probabilistic. Therefore, we first discuss the computational complexity for the second decoding stage. To evaluate the complexity of the second decoding stage, we perform a simulation to obtain the ensemble average of the cardinality of the subset $\mathcal{D}$, $\langle |\mathcal{D}| \rangle$, which corresponds to the average number of Euclidean distance calculations required to solve the problem given by (26). The results are shown in Figure 7, where $\binom{M_c}{M_p}$ and E_b/N_0 are chosen to be $\binom{16}{8}$ and 8 dB, respectively. Other specifications of the simulations can be seen in Table 2. Figure 7 shows that $\langle |\mathcal{D}| \rangle$ decreases with increasing $\Delta f T_s$ and M, and that $\langle |\mathcal{D}| \rangle$ is independent of the value of $\Delta f T_s$ if $\Delta f T_s \gtrsim 0.5$ for $M \geq 5$, where the curves are slightly nonmonotonic.

Figure 8 shows the total complexity of the proposed two-stage decoding algorithm relative to the complexity of ML decoding as a function of $\Delta f T_s$. The complexity is defined by the total number of calculations of the Euclidean distance required to obtain $\hat{\mathbf{x}}_{\mathcal{B}}$ and $\check{\mathbf{x}}_{\mathcal{B}}$. Figure 8 shows that for larger values of $\Delta f T_s$, the complexity remains constant[b] and takes a smaller value. For example, the complexity can be reduced to 3 to 6% of the complexity of ML decoding when $\Delta f T_s \gtrsim 0.5$ and $M = 4$ or 5.
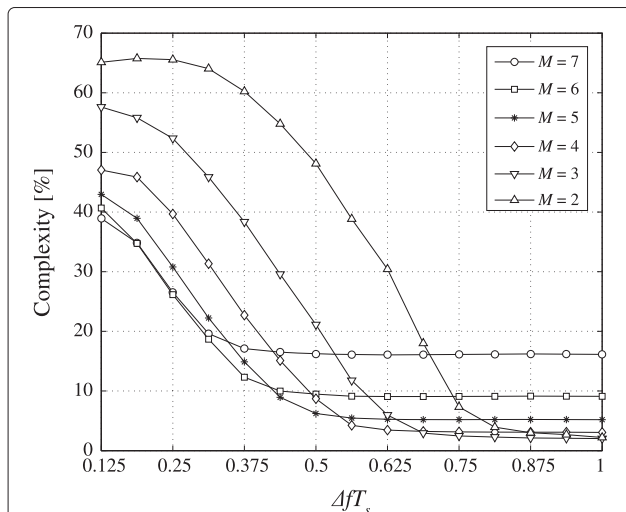

Figure 8 Total complexity of the two-stage decoding algorithm ($\binom{M_c}{M_p} = \binom{16}{8}$, $E_b/N_0 = 8$ dB).
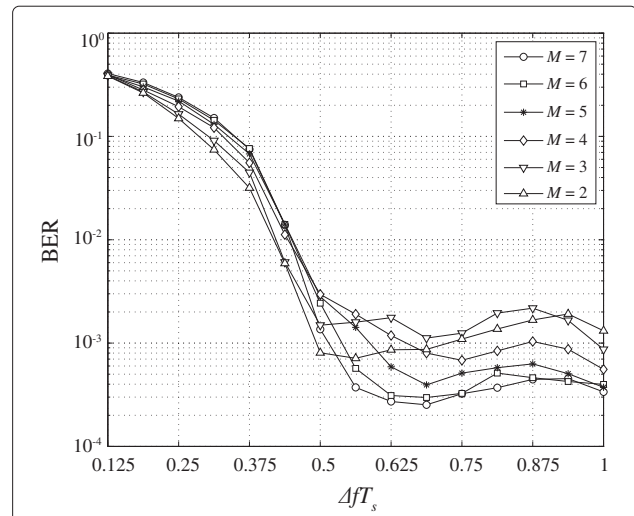

Figure 9 BER versus $\Delta f T_s$ for PC/HC-MCM using the two-stage decoding algorithm ($\binom{M_c}{M_p} = \binom{16}{8}$, $E_b/N_0 = 8$ dB).
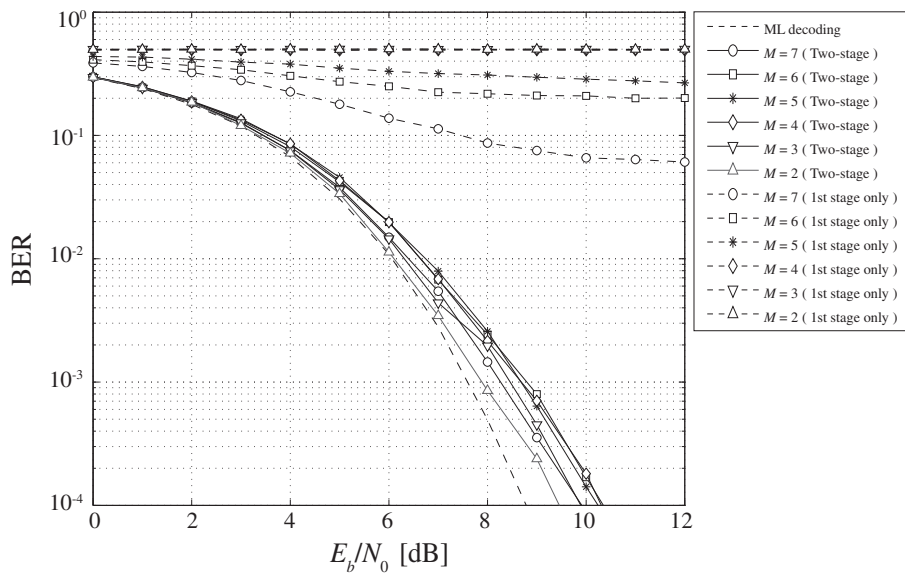
Figure 10 BER performance of PC/HC-MCM using the two-stage decoding algorithm $\left(\binom{M_c}{M_p} = \binom{16}{8}\right)$, $\Delta f T_s = 0.5$).

4.2 BER performance

The BER versus $\Delta f T_s$ characteristics for PC/HC-MCM using the proposed two-stage decoding algorithm are shown in Figure 9 for $E_b/N_0 = 8$ dB. It can be observed that the BER curves in Figure 9 exhibit some fluctuation when $\Delta f T_s \geq 0.5$. This is caused by intercarrier interference (ICI), which depends on the value of $\Delta f T_s$. Figure 10 shows the BER versus E_b/N_0 characteristics, where solid lines denote the results of the proposed decoding algorithm and dashed lines denote the results of ML decoding with the first decoding stage only. Figure 10 shows that the BER characteristics of PC/HC-MCM using the proposed decoding algorithm have a loss of less than approximately 1.5 dB in E_b/N_0 at a BER of 10^{-3} as compared with that of PC/HC-MCM using ML decoding. However, as shown in Figure 8, the computational complexity is greatly reduced by the proposed algorithm. It can be seen from Figure 10 that the best performance of the two-stage decoding algorithm is obtained with $M = 2$, for which the second decoding stage is dominant and the total computational complexity is the highest, even though the computational complexity of the first decoding stage using the (M)-algorithm is the lowest.

5 Conclusion

A decoding algorithm that consists of two decoding stages to reduce the complexity of decoding for PC/HC-MCM signals was proposed. The proposed two-stage decoding algorithm was demonstrated to be effective for reducing the computational complexity with only a small increase in BER. According to results obtained considering the equalization at the receiver [11], we believe that our proposed two-stage decoding algorithm can also be used in intersymbol interference (ISI) channels. In the near future, we will take the multipath and other ISI channels into consideration to develop a lower-complexity decoding algorithm for PC/HC-MCM.

Endnotes

[a]In the ordinary M-algorithm, the parameter M is used to limit maximum number of surviving branches. In this article, we only choose a single surviving branch to reduce the complexity, and M is the number of bits considered at each step. Thus, the meaning of the parameter M is different from that in the ordinary M-algorithm.

[b]As was shown in Figure 7, the complexity curves of $\langle |\mathcal{D}| \rangle$ for $\Delta f T_s \geq 0.5$ and $M = 4$ or 5 are nonmonotonic. However, such nonmonotonic behavior cannot be seen in Figure 8 because in the nonmonotonic parts in Figure 8, the complexity of the first decoding stage is dominant and the nonmonotonic behavior cannot be distinguished.

References
1. M Itami, Fundamentals of OFDM and its application. Fundament. Rev. **1**(2), 35–43 (2007)
2. RV Nee, R Prasad, *OFDM for Wireless Multimedia Communications*. (Artech House, Boston, 2000)
3. L Hanzo, M Munster, BJ Choi, T Keller, *OFDM and MC-CDMA for Broadband Multi-user Communications, WLANs and Broadcasting*. (Wiley, West Sussex, 2003)

4. J Zhu, S Sasaki, G Marubayashi, Proposal of parallel combinatory spread spectrum communication system. IEICE Trans. Commun. **J74-B**(5), 207–214 (1991)
5. S Sasaki, H Kikuchi, J Zhu, G Marubayashi, Multiple access performance of parallel combinatory spread spectrum communication systems in nonfading and Rayleigh fading channels. IEICE Trans. Commun. **E78-B**(8), 1152–1161 (1991)
6. SY Park, SB Yun, CG Kang, Performance of multi-carrier parallel combinatory DS-CDMA system. IEICE Trans. Commun. **E81-B**(9), 1758–1769 (1998)
7. K Takizawa, S Sasaki, S Muramatsu, J Zhou, H Kikuchi, Performance bounds in convolutional coded parallel combinatorial SS systems. IEICE Trans. Fundament. **E85-A**(7), 1696–1701 (2002)
8. K Ohuchi, Constant amplitude signaling for parallel combinatory spread spectrum systems. IEICE Trans. Fundament. **E89-A**(9), 2329–2336 (2006)
9. PK Frenger, N Arne, B Svensson, Parallel combinatory OFDM signaling. IEEE Trans. Commun. **47**(4), 558–565 (1999)
10. M Hamamura, S Tachikawa, in *Proceedings of the 15th IEEE International Symposium on Personal, Indoor and Mobile Radio Communications*, vol. 1. Bandwidth efficiency improvement for multi-carrier systems, (IEEE, Barcelona, 2004), pp. 48–52
11. Y Hou, M Hamamura, A novel modulation with parallel combinatory and high compaction multi-carrier modulation. IEICE Trans. Fundament. **E90-A**(11), 2556–2567 (2007)
12. G Ungerboeck, Adaptive maximum-likelihood receiver for carrier-modulated data-transmission systems. IEEE Trans. Commun. **20**(5), 624–636 (1974)
13. S Takahashi, M Hamamura, S Tachikawa, in *Proceedings of the 1st International Symposium on Wireless Communications Systems*, vol. 1. A demodulation complexity reduction method using M-algorithm for high compaction multicarrier modulation systems (University of Bristol, Mauritius, 2004), pp. 418–422
14. Y Morishige, M Fujii, M Itami, K Itoh, Tree search detection based on LLR Using M algorithm in MC-CDMA systems. IEICE Trans. Fundament. **E89-A**(10), 2622–2629 (2006)
15. K Adachi, M Nakagawa, Iterative modified QRD-M based on CRC codes for OFDM MIMO multiplexing. IEICE Trans. Commun. **E90-B**(6), 1433–1443 (2007)
16. KJ Kim, Jlltis Yue R A, JD Gibson, A QRD-M/Kalman filter-based detection and channel estimation algorithm for MIMO-OFDM systems. IEEE Trans. Wirel. Commun. **4**(2), 710–721 (2005)
17. JB Anderson, S Mohan, Sequential coding algorithms: a survey and cost analysis. IEEE Trans. Commun. **32**(2), 169–176 (1984)
18. R Hayashi, M Hamamura, in *Proceedings of the 5th International Conference on Innovations in Information Technology*, vol. 1. Complexity-reduced decoding algorithm for unmodulated parallel-combinatory high-compaction multicarrier modulation signals (IEEE, Al Ain, 2008), pp. 49–53
19. AH Nuttall, F Amoroso, Minimum Gabor bandwidth of *M*, orthogonal signals. IEEE Trans. Inf. Theory. **11**(3), 440–444 (1965)